

Long-term Periodicities in North–South Asymmetry of Solar Activity and Alignments of the Giant Planets

J. Javaraiah

© Springer

Abstract The existence of ≈ 12 -year and ≈ 51 -year periodicities in the north–south asymmetry of solar activity is well known. However, the origin of these as well as the well-known relatively short periodicities in the north–south asymmetry is not yet clear. Here we have analyzed the combined daily data of sunspot groups reported in Greenwich Photoheliographic Results (GPR) and Debrecen Photoheliographic Data (DPD) during the period 1874–2017 and the data of the orbital positions (ecliptic longitudes) of the giant planets in ten-day intervals during the period 1600–2099. Our analysis suggests that ≈ 12 -year and ≈ 51 -year periodicities in the north–south asymmetry of solar activity are the manifestations of the differences in the strengths of ≈ 11 -year and ≈ 51 -year periodicities of activity in the northern- and southern-hemispheres. During the period 1874–2017 the Morlet wavelet power spectrum of the north–south asymmetry of sunspot-group area and that of the mean absolute difference ($\overline{\psi_D}$) of the orbital positions of the giant planets are found to be similar. Particularly, there is a suggestion that the ≈ 12 -year and ≈ 51 -year periodicities in the north–south asymmetry of sunspot-group area occurred during approximately the same times as the corresponding periodicities in $\overline{\psi_D}$. Therefore, we suggest that there could be influence of some specific configurations of the giant planets in the origin of the ≈ 12 -year and ≈ 50 -year periodicities of the north–south asymmetry of solar activity.

Keywords: Sun: Dynamo – Sun: Solar activity – (Sun): Solar system dynamics

1. Introduction

The existence of the ≈ 12 -year and 40–50-year periodicities in the north–south asymmetry of solar activity has been reported by a number of authors. Carbonell, Oliver, and Ballester (1993) analyzed the combined GPR (1874–1983) and United States Air Force (1983–1989) data of sunspot groups and found that

#58, Bikasipura (BDA Layout), Bengaluru-560111, India.
Formerly working at Indian Institute of Astrophysics,
Bengaluru-560 034, India.
email: jajj55@yahoo.co.in;jdotjavaraiah@gmail.com

only a 12.1-year periodicity is statistically significant in the north–south asymmetry of sunspot area. Yi (1992) was first to point out that in the north–south asymmetry, derived by using the conventional formula $\frac{N-S}{N+S}$ (relative asymmetry), the 11–12-year periodicity is mostly an artifact of the 11-year cycle of the denominator $N+S$, where N and S are the quantities of the activity in northern and southern hemispheres, respectively. Javaraiah and Gokhale (1997) verified this by determining separately the power spectra of the $\frac{N-S}{N+S}$ and the $N-S$ (absolute asymmetry) of the sunspot data. They found that a peak at $\approx \frac{1}{12} \text{ year}^{-1}$ frequency in the power spectrum of $N-S$ is statistically insignificant and the same peak in the spectrum of $\frac{N-S}{N+S}$ is statistically very significant (see Figure 7 in Javaraiah and Gokhale, 1997). Obviously, they have confirmed the doubt of Yi (1992). Ballester, Oliver, and Carbonell (2005) have done the same. However, the statistical error in the relative asymmetry, $\frac{N-S}{N+S}$, is much smaller than that of the absolute asymmetry, $N-S$ (Javaraiah and Gokhale, 1997). Therefore, variations of the relative asymmetry could be more reliable than those of the absolute asymmetry. Javaraiah and Gokhale (1997) have also shown the existence of ≈ 50 -year periodicity in both the relative asymmetry and the absolute asymmetry, and a 8–9-year periodicity in the absolute asymmetry. Similar periods were also noticed by Ballester, Oliver, and Carbonell (2005). Knaack *et al.* (2004) by using a wavelet analysis, studied the long-term periodicities in the north–south asymmetry of the monthly averaged sunspot areas (1874–2003) and found the existence of the ≈ 12 -year and ≈ 43 -year periodicities in the relative asymmetry of the sunspot area. Similar periodicities in the relative north–south asymmetry of the areas of different size sunspot groups were also seen by Mandal and Banerjee (2016), using the Kodaikanal white-light digitized archive sunspot observations (1921–2011). Deng *et al.* (2016) from the wavelet analysis of sunspot areas of Solar Cycles 9–14 found the existence of ≈ 9 -year and ≈ 51 -year periodicities in both the relative asymmetry and the absolute asymmetry of sunspot area, and a ≈ 12 -year periodicity in the relative asymmetry only. Recently, Javaraiah (2019) studied cycle-to-cycle modulations in the relative north–south asymmetry of solar-cycle maximum and minimum and found that there exists a 30–50-year periodicity in the asymmetry of minimum and a possibility of the existence of a much longer (mostly substantially more than 100 years) periodicity in the asymmetry of maximum. Overall, the existence of 8–12-year and 40–50-year periodicities in the north–south asymmetry of solar activity is somewhat established from observational studies. Verma (1993) detected the existence of a 110-year periodicity in the relative north–south asymmetry of solar activity (also see Li *et al.*, 2002; Li *et al.*, 2019). Badalym and Obridko (2011) by using the method of Spectral Variation Analysis found the existence of long periods of phase shifts between northern- and southern-hemisphere’s activity.

The physical reason of the long periodicities as well as the well-known relatively short periodicities (170–180-day, 320–329-day, 1.5-year, 1.8-year, 2.1-year, 3.6-year, *etc.*; see Knaack *et al.*, 2004; Ravindra and Javaraiah, 2015 and the references therein) in the north–south asymmetry is not yet clear. Recently, Schüssler and Cameron (2018) showed that around 8.5-year and 30–50-year periods in the absolute asymmetry are the sum and beat periods of a 22-year period magnetic dipolar mode and a 13–15-year period quadrupolar

mode. Nepomnyashchikh *et al.* (2019) showed that long-term variations in the north–south asymmetry of solar activity resulting from short-term fluctuations in the α -effect of solar dynamo. On the other hand, a number of authors suggested the existence of a connection between solar variability (both long- and short-terms) and planetary configurations (Jose, 1965; Wood and Wood, 1965; Wood, 1972; Gokhale and Javaraiah, 1995; Zaqarashvili, 1997; Juckett, 2003; Wolff and Patrone, 2010; Abreu *et al.*, 2012; Cionco and Compagnucci, 2012; Wilson, 2013; Salvador, 2013; Sharp, 2013; Chowdhury *et al.*, 2016; Stefani *et al.*, 2016; Stefani, Giesecke, and Weier, 2019). Javaraiah (2005) found the existence of a good agreement between the amplitudes of the variations in the Sun’s spin and the orbital angular momenta at the common epochs of the steep decreases in both the orbital angular momentum and the Sun’s equatorial rotation rate determined from sunspot data. Since the Sun’s equator is inclined 7.17° to the ecliptic, the influences of configurations of the planets on solar activity may be different across the Sun’s equator (also see Juckett, 2000). Here we have analyzed the combined daily data of sunspot groups reported in GPR and DPD during the period 1874–2017 and the orbital positions (ecliptic longitudes) of the giant planets available for each ten-day interval during the period 1600–2099 and found that during the period 1874–2017 the Morlet wavelet power spectrum of the north–south asymmetry of sunspot-group area and that of the mean absolute difference ($\overline{\psi_D}$) of the orbital positions of the giant planets are similar. The wavelet spectra suggest that 12–13-year and the 40–50-year periodicities in the north–south asymmetry of sunspot-group area exist during approximately the same times as the corresponding periodicities in $\overline{\psi_D}$. Therefore, we suggest that there could be influence of some configurations of the giant planets in the origin of ≈ 12 -year and 40–50-year periodicities of the north–south asymmetry of solar activity.

In the next section we describe the data analysis, in Section 3 we present the results, and in Section 4 we summarize the conclusions and discuss them briefly.

2. Data analysis

Recently, Javaraiah (2019) analyzed the GPR and DPD sunspot-group daily data during the period April 1874– June 2017 (downloaded from fenyi.solarobs.unideb.hu/pub/DPD/) and derived the time series of the 13-month smoothed monthly mean corrected whole-spot areas of the sunspot groups in the Sun’s whole sphere (WSGA), northern hemisphere (NSGA), and southern hemisphere (SSGA). Here we have used these time series and derived the corresponding time series of both the relative north–south asymmetry (RNSA) and absolute north–south asymmetry (ANSA). The time series of the 13-month smoothed monthly mean values of the international sunspot number R_Z (ISSN) during the period 1874–2014 are downloaded from www.sidc.be/silso/datafiles (Source: WDC-SILSO, Royal Observatory of Belgium, Brussels). Here we have used the data on ecliptic longitudes (in degrees) ψ_J , ψ_S , ψ_U , and ψ_N of the giant planets Jupiter (J), Saturn (S), Uranus (U), and Neptune (N) in each 10-day interval during the period 1600–2099. These data were provided by Ferenc Varadi. He had derived these data

using the Jet Propulsion Laboratory (JPL) DE405 ephemeris (Seidelmann, 1992; Standish, 1998) for the period 1600–2099. We determined the average value ($\overline{\psi_D}$) of the absolute differences $|\psi_J - \psi_S|$, $|\psi_J - \psi_U|$, $|\psi_J - \psi_N|$, $|\psi_S - \psi_U|$, $|\psi_S - \psi_N|$, and $|\psi_U - \psi_N|$ in each ten-day interval during the period 1600–2099. The values of the absolute differences that are greater than 180° are converted as 360° minus the absolute difference. This is because of here we use minimum unsigned difference between the ecliptic longitudes (have values $0^\circ - 360^\circ$) of any two planets (we have not done this in the preliminary results reported in Javaraiah, 2018, where we compared the variations in the amplitudes of solar cycles and $\overline{\psi_D}$). From the wavelet transformation both time and frequency localization can be obtained (for more detail see Torrance and Compo, 1998). We have used the IDL codes of Morlet wavelet power spectral analysis, cross-wavelet transformation (XWT), and wavelet coherence (WCOH) provided by Torrance and Compo (1998). We have downloaded these from paos.colorado.edu/research/wavelets. The cross-wavelet spectrum reveals localized similarity (covariance) in time and scale (period). WCOH is a normalized time and scale (period) resolved measure for the relationship between two time series (also see Marun and Kurths, 2016). A number of authors used XWT and WCO to study asynchronous behavior of northern and southern hemispheres activity (*e.g.*, Li *et al.*, 2010; Deng *et al.*, 2016, and the references therein). We made Morlet wavelet power spectral analysis of NSGA, SSGA, RNSA, and ANSA and compared the power spectra. We also made the Morlet wavelet spectral analysis of $\overline{\psi_D}$ and compared the wavelet power spectra of $\overline{\psi_D}$, RNSA, and ANSA. In addition, we have applied XWT and WCOH to the time series of these parameters to confirm the similarities seen in the Morlet wavelet power spectra of these parameters.

3. Results

Figure 1 shows the variations in the 13-month smoothed monthly mean WSGA, NSGA, and SSGA during the period 1874–2017, and the variation in ISSN (R_z) during the period 1874–2014. This figure is a slightly modified (clarity improved) version of the Figure 1 of Javaraiah (2019). Figure 2 shows the variations in the relative north–south asymmetry, RNSA, and in the absolute north–south asymmetry, ANSA, determined from the 13-month smoothed monthly mean NSGA and SSGA during the period 1874–2017. In this figure the variation in $\overline{\psi_D}$ values of ten-day intervals during the period 1874–2017 and the variation in ISSN during the period 1874–2014 are also shown. As can be seen in this figure, both the RNSA and the ANSA are considerably vary. The variation in RNSA is much more pronounced than that in ANSA. Obviously, the variations of RNSA and ANSA are considerably different. A major difference is during the minima of a majority of solar cycles RNSA is much larger than that of during the maxima. The behavior of ANSA is somewhat opposite to it. However, still there exists a high correlation between RNSA and ANSA (correlation coefficient $r = 0.63$). During the late Maunder minimum the activity pattern, *i.e.* the large north–south asymmetry in the activity (see Sokoloff and Nesme-Ribes, 1994) is consistent with the aforementioned behavior of RNSA. There are ≈ 11 -year cycles

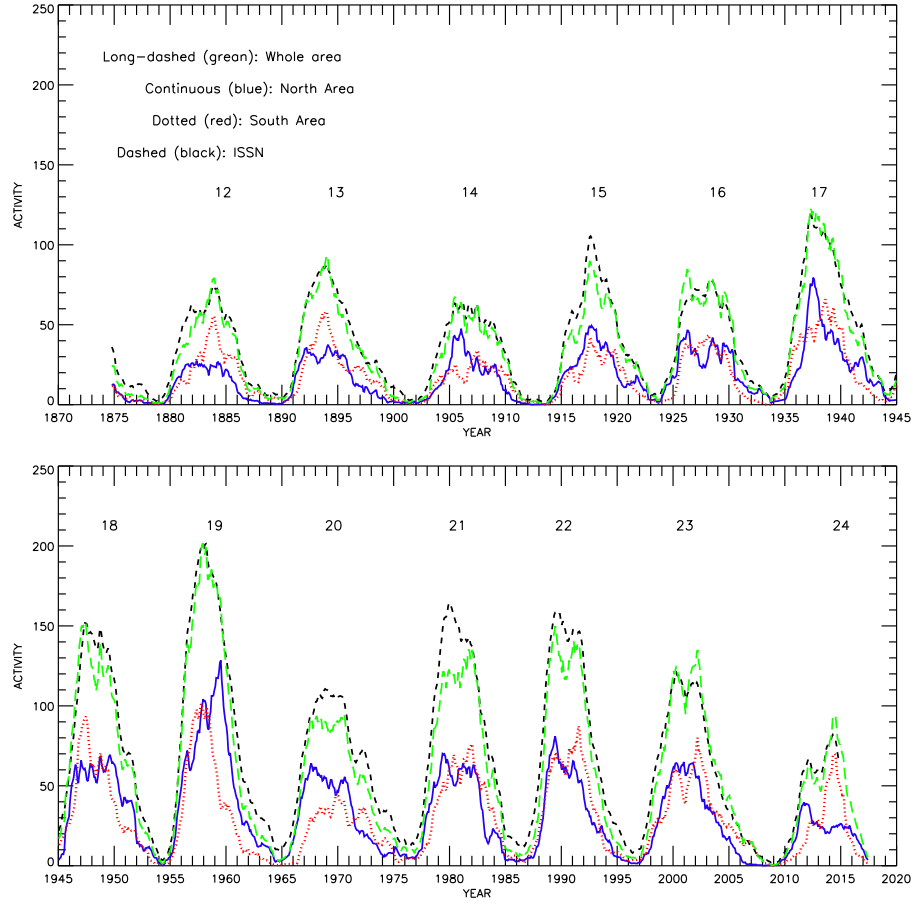


Figure 1. Variations in the 13-month smoothed monthly mean area of sunspot groups in the whole sphere: WSGA (*green-long-dashed curve*), northern hemisphere: NSGA (*blue-continuous curve*), southern hemisphere: SSGA (*red-dotted curve*) during the period 1874–2017, and international sunspot number (ISSN) R_z (*black-dashed curve*) during the period 1874–2014. The values of WSGA, NSGA, and SSGA are first divided by the largest value of WSGA, 3480.15 msh, and then multiplied by the largest value, 201.3, of ISSN. Waldmeier numbers of the solar cycles are also shown. This figure is a slightly modified (clarity improved) version of the Figure 1 of Javaraiah (2019).

in all RNSA, ANSA, and $\overline{\psi_D}$. However, there is a suggestion that no appreciable correlation between ISSN and any of the parameters RNSA, ANSA, and $\overline{\psi_D}$. There are patterns (around 1885–1955 and 1965–2015) of about 40–60-year cycles in $\overline{\psi_D}$. Such a pattern seems to exist also in RNSA and ANSA, but it is not visible clearly.

Figures 3a and 3b show the Morlet wavelet power spectra, and the corresponding global spectra, of NSGA and SSGA, respectively. As can be seen in these figures, obviously an ≈ 11 -year periodicity exists in both NSGA and SSGA and dominant almost throughout the period 1874–2017. There is also a suggestion on the existence of a relatively much weaker ≈ 50 -year periodicity in both the

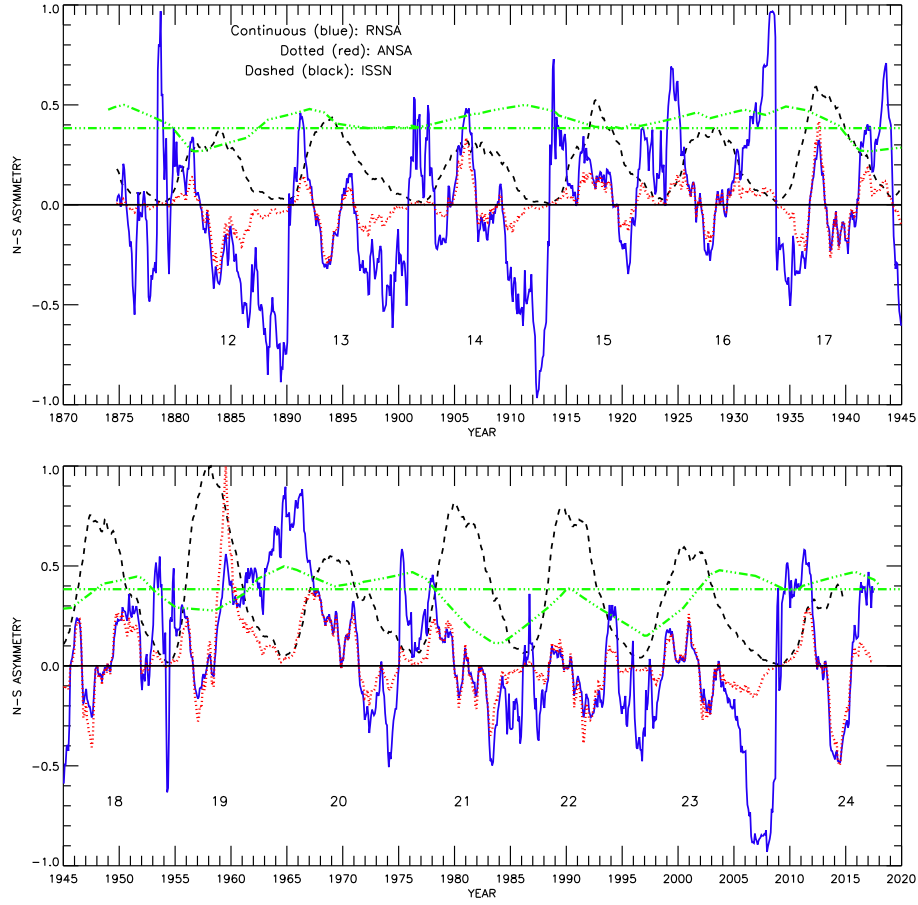


Figure 2. Variations in the relative north–south asymmetry: RNSA (*blue-continuous curve*) and absolute north–south asymmetry: ANSA (*red-dotted curve*) determined from 13-month smoothed monthly NSGA and SSGA during the period 1874–2017. The latter is divided by the maximum value (1593.61 msh) of the absolute ANSA. A positive (negative) value implies that the activity in northern (southern) hemisphere is higher than that of in southern (northern) hemisphere. The *black-dashed curve* represents the variation in the normalized international sunspot number (ISSN) R_z during the period 1874–2014 and the *green-dotted-dashed curve* represent the $\overline{\psi_D}$ in ten-day intervals during the period 1874–2017 (divided by two times of maximum value, 119.05°). Waldmeier numbers of the solar cycles are also shown.

NSGA and the SSGA, but after around 1920. In the Morlet wavelet and global spectra of WSGA, which are not shown here, besides the much stronger ≈ 11 -year periodicity, a very weak ≈ 50 -year periodicity is seen.

Figures 4a and 4b show the Morlet wavelet power spectra, and the corresponding global spectra, of the relative north–south asymmetry, RNSA, and the absolute north–south asymmetry, ANSA, respectively. As can be seen in these figures a ≈ 12.8 -year periodicity exists in RNSA and a ≈ 9.6 year periodicity exists in ANSA. However, there is a strong suggestion that each of these periods vary with time considerably (from 8 to 16 years) and systematically. That is, a large

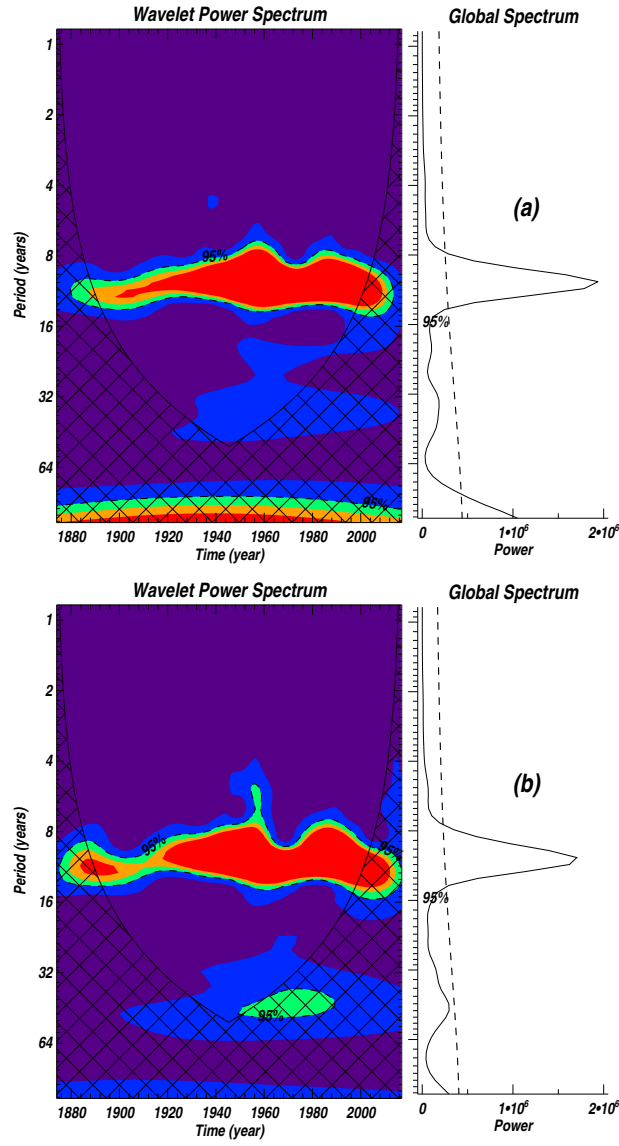


Figure 3. Panels (a) and (b) show the wavelet and global power spectra of NSGA and SSGA shown in Figure 1, respectively (power is divided by 10). The wavelet spectra are normalized by the variances of the corresponding time series. The shadings are at the normalized variances of 1.0, 3.0, 4.5, and 6.0. The *dashed curves* represent the 95% confidence levels deduced by assuming a white-noise process. The *cross-hatched regions* indicate the cone of influence where edge effects become significant (Torrence and Compo, 1998).

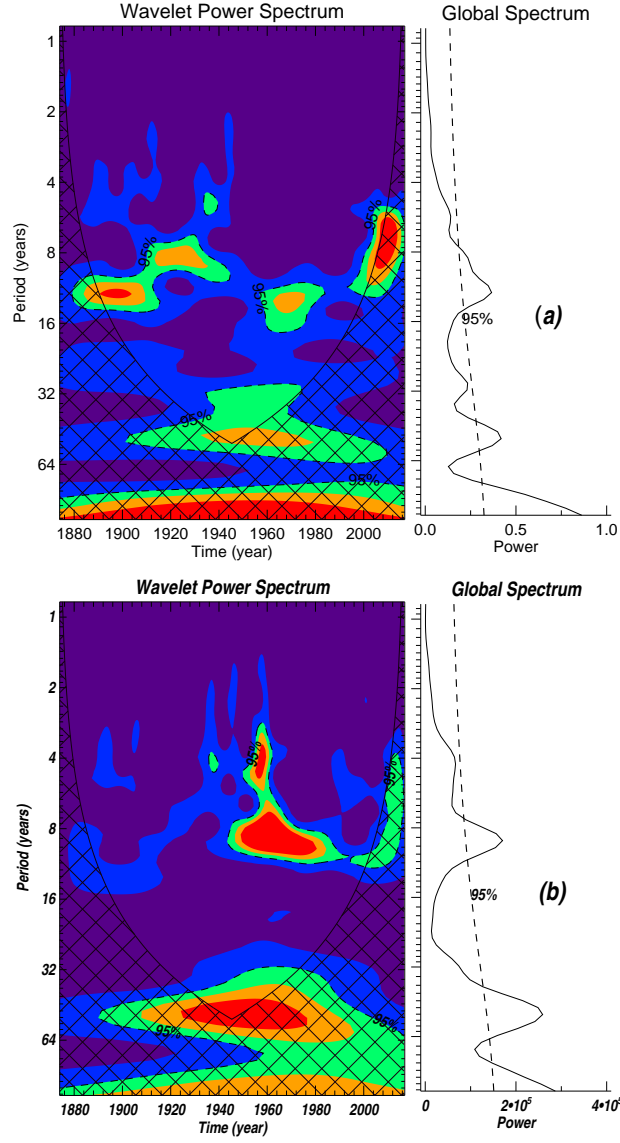


Figure 4. Panels (a) and (b) show the wavelet and global power spectra of RNSA and ANSA shown in Figure 2, respectively (power is divided by 10). The wavelet spectra are normalized by the variances of the corresponding time series. The shadings are at the normalized variances of 1.0, 3.0, 4.5, and 6.0. The *dashed curves* represent the 95% confidence levels deduced by assuming a white-noise process. The *cross-hatched regions* indicate the cone of influence where edge effects become significant (Torrence and Compo, 1998).

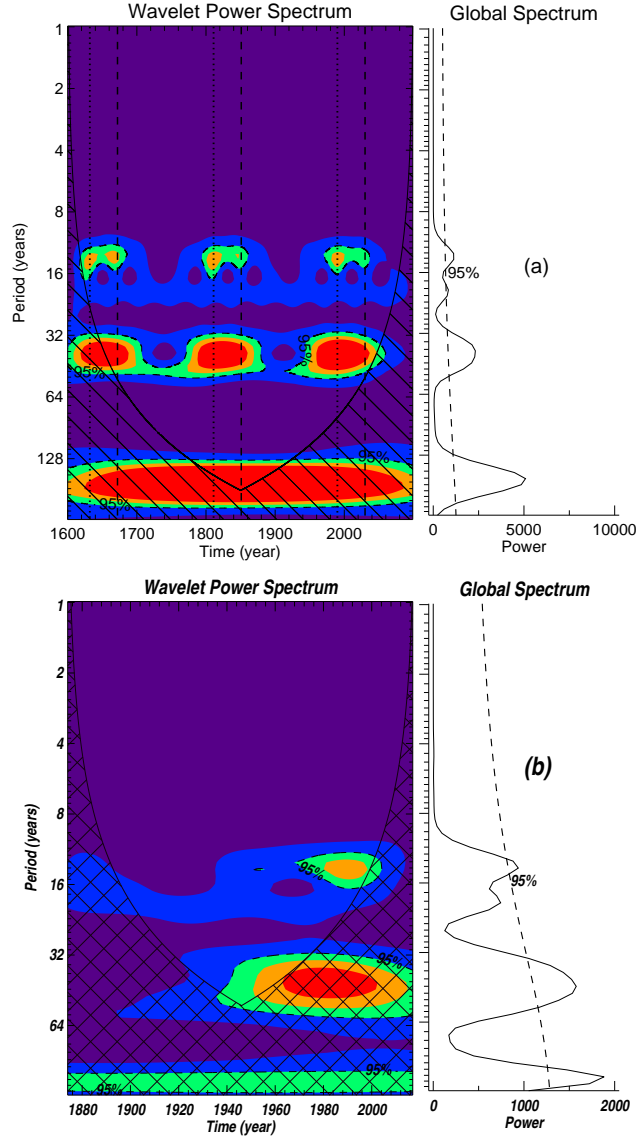


Figure 5. Panels (a) and (b) show the wavelet and global power spectra of $\overline{\psi_D}$ in ten-day intervals during the periods 1600–2099 and 1874–2017 (that is shown in Figure 2), respectively (power is divided by 100). The wavelet spectra are normalized by the variances of the corresponding time series. The shadings are at the normalized variances of 1.0, 3.0, 4.5, and 6.0. The *dashed curves* represent the 95% confidence levels deduced by assuming a white-noise process. The *cross-hatched regions* indicate the cone of influence where edge effects become significant (Torrence and Compo, 1998). The *dotted vertical lines* (at 1632, 1811, and 1990) and the *dashed vertical lines* (at 1672, 1851, and 2030) are drawn in the panel **a** at the epochs of the steep decreases in the orbital angular momentum of the Sun. There are some differences in the alignments of the giant planets at the locations of the *dotted* and the *continuous vertical lines* (see Javaraiah, 2005).

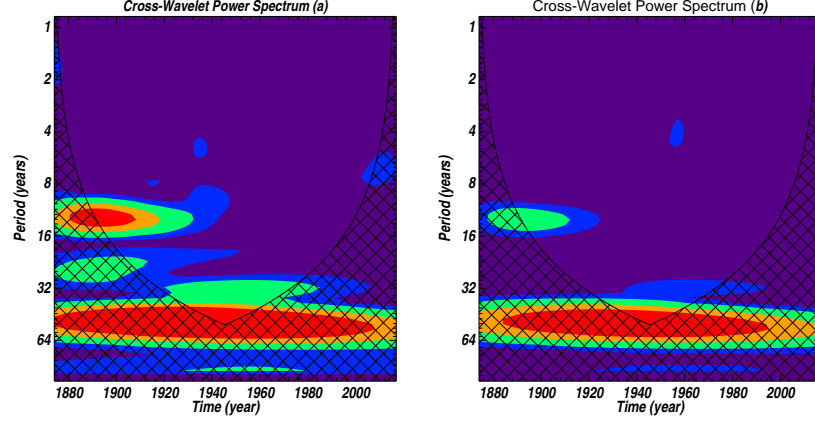


Figure 6. The panel (a) shows the cross-wavelet power spectra of RNSA and $\overline{\psi_D}$ and the panel (b) shows that of ANSA and $\overline{\psi_D}$ during 1874–2017 (in the case of panel b power is multiplied by 10^6). The shadings are at levels 1, 3, 10, and 20. The *cross-hatched regions* indicate the cone of influence where edge effects become significant (Torrence and Compo, 1998).

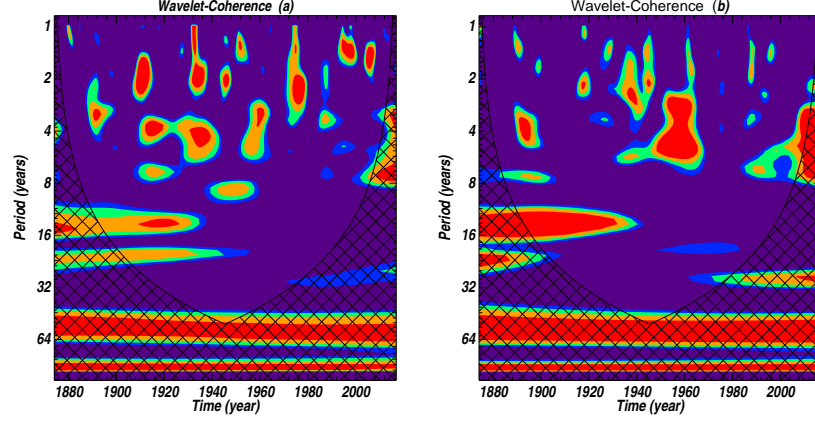


Figure 7. The panel (a) shows the wavelet-coherence (WCOH) of RNSA and $\overline{\psi_D}$ and the panel (b) shows that of ANSA (normalized) and $\overline{\psi_D}$ during 1874–2017. The shadings are at levels 0.5, 0.6, 0.7, and 0.8. A value of WCOH one means the existence of a linear relationship and zero means vanishing correlation. The *cross-hatched regions* indicate the cone of influence where edge effects become significant (Torrence and Compo, 1998).

change of this periodicity seems to be occurring in alternate 30–35 years, mainly in the case of RNSA. That is, in the case of RNSA a ≈ 12.8 -year periodicity was strong around the period 1880–1920, a ≈ 9 -year period was strong around the period 1920–1950, a ≈ 12.8 -year period was strong around the period 1960–1990, and then onwards a ≈ 9 -year periodicity is strong. Such clear alternate patterns are not present in ANSA, but overall variations in the ≈ 12.8 -year periodicity of RNSA and in the ≈ 9 -year periodicity of ANSA are the same. In ANSA the ≈ 9 -year periodicity was strong only around the period 1945–1985. There is a suggestion on the existence of a ≈ 51 -year periodicity (poorly resolved) in both

RNSA and ANSA and it was strongly present during the period 1900–1990. The global spectrum of RNSA suggests that the strengths of the ≈ 12.8 -year and the ≈ 51 -year periodicities in RNSA are almost equal (the former is only slightly weaker than the latter) in RNSA, whereas the global spectrum of ANSA suggests that in ANSA the ≈ 51 -year periodicity is considerably stronger than the ≈ 9 -year periodicity. Besides the existence of these periodicities, there are episodes of a 4–5-year periodicity in both RNSA and ANSA. This periodicity was strong in RNSA around 1960. Duchlev and Dermendjiev (1996) found a strong 35-year periodicity in the north–south asymmetry of solar filament activity during 1919–1989. A ≈ 32 -year periodicity is also present in RNSA (see Figure 4a), but it is relatively very weak.

As can be seen in Figure 3 in the global spectra the peak at ≈ 11 -year period of SSGA is slightly smaller than that of NSGA, whereas the peak of ≈ 50 -year period of SSGA slightly larger (close to the 95% confidence level) than that in NSGA (much less than 95% confidence level). Therefore, the ≈ 12.8 -year and ≈ 51 -year periodicities in RNSA and the ≈ 9 -year and ≈ 51 -year periodicities in ANSA are look to be resulted due to the aforementioned differences in the strengths of ≈ 11 -year and ≈ 50 -year periodicities in NSGA and SSGA. In addition, the approximate two year difference exists between the ≈ 12.8 -year/ ≈ 9 -year period of RNSA/ANSA and ≈ 11 -year period of NSGA and SSGA could be due to there exist 1–2 years differences in the positions (1–2-year phase difference) of the ≈ 11 -year peaks of NSGA and SSGA (*e.g.*, Norton and Gallagher, 2010; Javaraiah, 2019, also see Figure 1). Overall, the ≈ 12 -year and ≈ 51 -year periodicities in the north–south asymmetry of solar activity seem to be manifestations of the differences in the strengths of ≈ 11 -year and ≈ 51 -year periodicities of activity in northern- and southern-hemispheres. As already mentioned in Section 1, the statistical error in the relative asymmetry, RNSA, is much smaller than that of the absolute asymmetry, ANSA (see Javaraiah and Gokhale, 1997). Therefore, the variations of RNSA can be more reliable than the variations of ANSA. That is, the ≈ 12.8 -year and ≈ 51 -year periodicities of RNSA are more reliable than the ≈ 9 -year and ≈ 51 -year periodicities of ANSA.

Figure 5a shows the Morlet wavelet and global power spectra of $\overline{\psi_D}$ in ten-day intervals during the periods 1600–2099. In this figure the epochs of the steep decrease in the orbital angular momentum of the Sun are also shown (also see Javaraiah, 2005, 2017). Figure 5b shows the wavelet and global power spectra of $\overline{\psi_D}$ in ten-day intervals during the periods 1874–2017. We compare this figure with Figures 4a and 4b, *viz.* the wavelet spectra of RNSA and ANSA for the period 1874–2017. As can be seen in Figure 5a, there exist ≈ 13.6 -year and ≈ 41.6 -year periodicities in $\overline{\psi_D}$ around the years 1632, 1672, 1811, 1851, 1990, and 2030, when there was steep decrease in the Sun’s orbital angular momentum about the solar system barycenter caused by some specific configurations of the giant planets (see Javaraiah, 2005). The well-known 179-year period of the Sun’s orbital angular momentum (Jose, 1965) is obviously exists in $\overline{\psi_D}$ (however, most of the power spectral region of this period is within the region of cone of influence). In addition, relatively a very weak ≈ 20 -year periodicity exists in $\overline{\psi_D}$, continuously throughout the 1600–2099. The wavelet and the global spectra of RNSA and ANSA are somewhat closely match with that of $\overline{\psi_D}$ shown

Figure 5b. Particularly, there is a suggestion that the 12–13-year and 40–50-year periodicities in RNSA and ANSA were occurred during approximately the same times as the corresponding periodicities in $\overline{\psi_D}$. In the global spectra of both north–south asymmetry of sunspot area and $\overline{\psi_D}$ there is a suggestion that an increase of power with an increase in the value of period. That is, there is a suggestion that not only the values of the aforementioned periods of the north–south asymmetry of solar activity and $\overline{\psi_D}$ and their timings match, the relative powers of these periods are also approximately match. Therefore, we suggest that there could be influence of some specific configurations of the giant planets in the origin of ≈ 12 -year and 40–50-year periodicities of the north–south asymmetry of solar activity.

The power spectral area of the ≈ 51 periodicity in RNSA and ANSA is within the region of cone of influence in the corresponding wavelet power spectra. That is, the available 144 years data of sunspot groups used here are not adequate for accurately determining this periodicity in RNSA and ANSA from wavelet analysis. On the other hand, as can be seen in Figure 5a, the existence of a 40–50-year periodicity in $\overline{\psi_D}$ is very clear in the data during 1600–2099. In view of this, the corresponding periodicity in $\overline{\psi_D}$ obtained from the data during the period 1874–2017 may be reliable in spite of most of its power spectral area is within the region of the cone of influence. This may imply that the existence of this periodicity seen in the wavelet power spectra of RNSA and ANSA is mostly reliable. Moreover, the 50-year peaks in the Global power spectra of the north-south asymmetry are statistically significant on much more than 95% confidence level. This periodicity in north–south asymmetry of solar activity is found to be statistically significant in the fast Fourier transform and periodogram analyses (*e.g.*, Javaraiah and Gokhale, 1997; Deng *et al.*, 2016). The 40–50-year periodicity in $\overline{\psi_D}$ is not continuously present throughout the period 1600–2099 (see Figure 5a). In particular, as already mentioned above, this periodicity, and even the ≈ 12 -year periodicity, in $\overline{\psi_D}$ seem to present strongly around the epochs where the Sun’s orbital motion is retrograde. Hence, around such occasions the ≈ 12 -year and ≈ 51 -year periodicities may be occurring and strong in the north–south asymmetry of solar activity.

Figures 6a and 6b show the cross-wavelet power spectrum of RNSA and that of $\overline{\psi_D}$ and ANSA and $\overline{\psi_D}$, respectively, during the period 1874–2017. These figures indicate a large similarities (covariance) exist between the time series of $\overline{\psi_D}$ and north–south asymmetry in sunspot-group area at scale (period) ≈ 12 -year mainly before 1940 and at the scale (period) ≈ 51 -year throughout 1874–2017. Figures 7a and 7b show the wavelet-coherence of RNSA and $\overline{\psi_D}$ and that of ANSA (normalized) and $\overline{\psi_D}$, respectively, during the period 1874–2017. In these figures there is a suggestion that the wavelet-coherence exists between $\overline{\psi_D}$ and north–south asymmetry of solar activity at most of the known periodicities (including 1.5-year, 1.8-year, 2.1-year, 3.6-year, *etc.*) of the latter, at several times. However, in WCOH spectra spurious peaks can occur for the areas of low wavelet power (Marun and Kurths, 2016). On the other hand, the wavelet-cross spectrum may not suitable for significance testing the interrelation between two processes. Therefore, wavelet-coherence may be very useful (Marun and Kurths, 2016). Nevertheless, the wavelet cross spectra (Figures 6a

and 6b), and even the WCOH spectra (Figures 7a and 7b), suggest that in the case of ≈ 12 -year periodicity, only before 1940 a large similarity (covariance) exists between the time series of $\overline{\psi_D}$ and north-south asymmetry in sunspot-group area. In addition, the spectral region of ≈ 51 -year periodicity is within the region of cone of influence. Therefore, the inference above, *i.e.* the influence of some specific configurations of the giant planets in the origin of ≈ 12 -year and ≈ 51 -year periodicities of north–south asymmetry of solar activity is only suggestive rather than compelling.

4. Conclusions and Discussion

The existence of ≈ 12 -year and ≈ 51 -year periodicities in the north–south asymmetry of solar activity seems to be established to some extent by now from observational point of view. However, the physical reason of these as well as the known relatively short periodicities in the north–south asymmetry is not yet clear. Here we have analyzed the combined daily data of sunspot groups reported in GPR and DPD during the period 1874–2017 and the data of the orbital positions (ecliptic longitudes) of the giant planets in ten-day intervals during the period 1600–2099. Our analysis suggests that the ≈ 12 -year and ≈ 51 -year periodicities in the north–south asymmetry of solar activity could be manifestations of the differences in the strengths of ≈ 11 -year and ≈ 51 -year periodicities of activity in northern- and southern-hemispheres. During the period 1874–2017 the Morlet wavelet power spectra of the north–south asymmetry of sunspot-group area and the mean absolute difference ($\overline{\psi_D}$) of the orbital positions of the giant planets are found to be similar. Particularly, the wavelet spectra suggest that the 12–13-year and 40–50-year periodicities in the north–south asymmetry of sunspot area occurred during approximately the same times as the corresponding periodicities in $\overline{\psi_D}$. In addition, the relative powers of these periods of the north–south asymmetry and $\overline{\psi_D}$ are also found to be matched. Therefore, we suggest that there could be influence of some specific configurations of the giant planets in the origin of the 12–13-year and 40–50-year periodicities in the north–south asymmetry of solar activity.

Depending on the torque acting on the system, the angular momentum of the system might be conserved in only one or two directions but not all the directions. The net torque on the Sun (an extended body) due to gravitational force of the planets may not be always zero, though it is small. That is, there could be some changes in the solar differential rotation rate due to the external forces on the Sun (*e.g.*, Zaqarashvili, 1997) and hence, in the strength of solar dynamo, suggesting planetary configurations have an influence in solar variability. However, a planetary influence on solar activity, even if it exists, seems to be negligibly small (De Jager and Versteegh, 2005). There is a continuous progress on this topic. Abreu *et al.* (2012) suggested that variations in solar rotation through time-dependent torque exerted by the planets on the non-spherical solar tachocline responsible for the solar cycle and other variations of solar activity. Wilson (2013) constructed a Venus–Earth–Jupiter spin–orbit coupling model. According to this model net tangential torques due to time

dependent alignments of Venus, Earth, and Jupiter act upon the outer convective layers of the Sun with periodicities that match many of the long-term solar cycles. Stefani *et al.* (2016) and Stefani, Giesecke, and Weier (2019) have shown that tidal force induced by the Venus–Earth–Jupiter system affect solar dynamo through resonant excitation of the oscillation of the α -effect.

When the Sun’s orbital angular momentum was close to zero (the Sun was close to the barycenter), the solar equatorial rotation rate was also considerably low (the steep decreases in the Sun’s spin and orbital angular momenta have the same value, $\approx 10^{47}$ g cm² s⁻¹; see Javaraiah, 2005), suggesting that the differential rotation rate was considerably low, *i.e.* a weak dynamo. That is, at least the Sun’s retrograde orbital motion about the solar system barycenter may influence the solar dynamo and may be responsible for the grand minima, such as Maunder minimum (also see Cionco and Compagnucci, 2012). Although the altitude of planetary tidal waves on the Sun is of the order of only one millimeter (*e.g.*, Condon and Schmidt, 1975), it may be enlarged appreciably at the times of some alignments of the Jupiter with other planets. There may be a complicated coupling between the variation in the rotation rate caused by some specific alignments of the tide rising planets (Venus, Earth, and Jupiter) and the variation in the orbital motion of the Sun due to some specific alignments of the giant planets. Depending on the differences among the angular inclinations of the orbits of planets to the ecliptic (in the heliocentric co-ordinate system), during a specific configuration of planets the maximum angular distances of the planets above and below the ecliptic (or invariant plane) cause the maximum north–south asymmetry in the distribution of mass and angular momentum in the solar system. Javaraiah (2003) showed the presence of the periods of the alignments of two or more giant planets in both the solar differential rotation and its north–south asymmetry determined from the sunspot-group data during the period 1879–1976. As suggested by Gokhale and Javaraiah (1995), variations in the north–south asymmetry of solar activity may represent anti-symmetric global modes of solar magnetic oscillations and the perturbations needed for all the global modes of solar magnetic oscillations may be provided by some specific configurations of the planets. Moreover, besides there exists a considerable north–south asymmetry in both the solar differential rotation and the meridional flow, a reasonable correlation also exists between solar cycle variations of the differential rotation rate and the meridional motion of sunspot groups (Javaraiah and Ulrich, 2006). Shirley (2017) found the existence of a highly statistical significant correlation between the solar meridional flow and the Sun’s orbital torque during the Solar Cycle 23. Recent numerical simulations from a flux transport dynamo model show importance of time variation and north–south asymmetry in meridional circulation in producing differing solar cycles in the northern- and southern-hemispheres (Belucz and Dikpati, 2013). We think that the effect of differences in the time-dependent configurations of planets above and below the ecliptic may be responsible for variations in the north–south asymmetry of solar differential rotation and meridional circulation that are in turn responsible for the variations of north–south asymmetry in solar activity.

5. Acknowledgments

The author thanks anonymous referee for helpful comments and suggestions. The author is thankful to Ferenc Varadi for providing the entire planetary data used here. Wavelet software was provided by C. Torrence and G. Compo and is available at <http://paos.colorado.edu/research/wavelets>.

6. Disclosure of Potential Conflicts of Interest

The author declares that he has no conflicts of interest.

References

- Abreu, J.A., Beer, J., Ferriz-Mas, A., McCracken K.G., Steinhilber, F.: 2012, *Astron. Astrophys.* **548**, A88. DOI: 10.1051/0004-6361/20219997
- Ballester, J.L., Oliver, R., Carbonell, M.: 2005, *Astron. Astrophys.*, **431**, L5. DOI: 10.1951/0004-6361:200400135
- Badalyan, O.G., Obridko, V.N.: 2011, *New Astron.* **16**, 357. DOI: 10.1016/j.newast.2011.01.005
- Belucz, B., Dikpati, M.: 2013, *Astrophys. J.* **779**, 4. DOI: 10.1088/0004-1075637X/779/1/4
- Carbonell, M., Oliver, R., Ballester, J.L.: 1993, *Astron. Astrophys.* **274**, 497. DOI: 10.3847/0004-6256/151/3/70
- Chowdhury, P., Gokhale, M.H., Singh, J., Moon, Y.-J.: 2016, *Astrophys. Space Sci.*, **361**, 54. DOI: 10.1007/s10509-015-2641-8
- Cionco, R.G., Compagnucci, R.H.: 2012, *Adv. Space Res.* **50**, 1434. DOI: 10.1016/j.asr.2012.07.013
- Condon, J.J., Schmidt, R.R.: 1975, *Solar Phys.* **42**, 529. DOI: 10.1007/BF00149930
- De Jager, C., Versteegh, G.: 2005, *Solar Phys.* **229**, 175. DOI: 10.1007/s11207-005-4086-7
- Deng, L.H., Xiang, Y.Y., Qu, Z.N., An, J.M.: 2016, *Asrophys. J.* **151**, 70. DOI: 10.3847/0004-6256/151/3/70
- Duchlev, P.I., Dermendjiev, V.N.: 1996, *Solar Phys.* **168**, 205. DOI: 10.1007/BF00145836
- Gokhale, M.H., Javaraiah, J.: 1995, *Solar Phys.* **156**, 157. DOI: 10.1007/BF00669582
- Javaraiah, J.: 2003, *Solar Phys.* **212**, 23. DOI: 10.101023/A:1022912430585
- Javaraiah, J.: 2005, *Mon. Not. Roy. Astron. Soc.* **362**, 1311. DOI: 10.1111/j.1365-2966.2005.09403.x
- Javaraiah, J.: 2017, *Solar Phys.* **292**, 172. DOI: 10.1007/s11207-017-1197-x
- Javaraiah, J.: 2018, In: Dr. Banerjee, J., Jiang, K., Kusano, S., Solanki, eds., Long-Term Datasets for the Understanding of Solar and Stellar Magnetic Cycles, *Proc. IAU Symp.*, No. 340, P.263. DOI: 10.1017/S1743921318001321
- Javaraiah, J.: 2019, *Solar Phys.* **294**, 64. DOI: 10.1007/s11207-019-442-6
- Javaraiah, J., Gokhale, M.H.: 1997, *Solar Phys.* **170**, 389. DOI: 10.1023/A:1004928020737
- Javaraiah, J., Ulrich, R.K.: 2006, *Solar Phys.* **237**, 245. DOI: 10.1007/s11207-006-0130-5
- Jose P.D.: 1965, *Astronomic. J.* **70**, 193. DOI: 10.1086/109714
- Juckett, D.A.: 2000, *Solar Phys.* **191**, 201. DOI: 10.1023/A:1005226724316
- Juckett, D.A.: 2003, *Astron. Astrophys.* **399**, 731. DOI: 10.1051/0004-6361:20021923
- Knaack, R., Stenflo, J.O., Berdyugina, S.V.: 2004, *Astron. Astrophys.* **418**, L17. DOI: 10.1051/0004-6361:20040107
- Li, F.Y., Wang, J.X., Xiang, N.B., Xie, J.L., Xu, J.C.: 2019, *Astrophys. J.* **873**, 121. DOI: 10.3847/1538-4357/ab06bf
- Li, K.J., Gao, P.X., Zhan, L.S., Shi, X.J., Zhu, W.W.: 2010, *Mon. Not. R. Astron. Soc.*, **401**, 342. DOI: 10.1111/j.1365-2966.2009.15639.x
- Li, K.J., Wang, J.X., Xiong, S.Y., Liang, H.F., Yun, H.S., Gu, X.M.: 2002, *Astron. Astrophys.* **383**, 648. DOI: 10.1051/0004-6361:20011799
- Mandal, S., Banerjee, D.: 2016, *Astrophys. J. Lett.* **830**, L33. DOI: 10.3847/2041-8205/830/2/L33

- Maraun, D., Kurths, J.: 2004, *Nonlin. Proc. in Geophys.*, **11**, 505. SRef-ID: 1607-7946/npg/2004-11-505.
- Nepomnyashchikh, A., Mandal, S., Banerjee, D., Kitchatinov, L.: 2019, *Astron. Astrophys.* **625**, A37. DOI: 10.1051/0004-6361/201935224
- Norton, A.A., Gallagher, J. C.: 2010, *Solar Phys.* **261**, 193. DOI: 10.1007/s11207-009-9479-6
- Ravindra, B., Javaraiah, J.: 2015, *New Astron.* **39**, 55. DOI: 10.1016/j.newast.2015.03.004
- Schüssler, M., Cameron, R.H.: 2018, *Astron. Astrophys.*, **618**, A89. DOI: 10.1051/0004-6361/201833532
- Salvador, R.J.: 2013, *Pattern Recogn. Phys.* **1**, 117. DOI: 10.5194/prp-1-117-2013
- Seidelmann, P.K.: 1992, *Explanatory supplement to The Astronomical Almanac*, revised edition. University Science Books, MillValley, CA, USA.
- Sharp, G.J.: 2013, *Int. J. Astron. Astrophys.*, **3**, 260. DOI: 10.4236/ijaa.2013.33031
- Shirley, J.H.: 2017, arXiv:1706.01854.
- Sokoloff, D., Nesme-Ribes, E.: 1994, *Astron. Astrophys.* **288**, 293.
- Standish, E.M.: 1998, *JPL Planetary and Lunar Ephemerides*, DE405/LE405, Interoffice Memo. 312.F-98-048. Jet Propulsion Laboratory, Pasadena, CA, 1998. (ftp://navigator.jpl.nasa.gov/ephem/export/de405.iom)
- Stefani, F., Giesecke, A., Weier, T.: 2019, *Solar Phys.* **294**, 60. DOI: 10.1007/s11207-019-1447-1
- Stefani, F., Giesecke, A., Weber, N., Weier, T.: 2016, *Solar Phys.* **291**, 2197. DOI: 10.1007/s11207-016-0968-0
- Torrence, Ch., Compo, G.P.: 1998, *Bull. Am. Meteor. Soc.* **79**, 61. DOI: 10.1175/1520-0477(1998)079<0061,APGTWA>2.0.CO;2
- Verma, V.K.: 1993, *Astrophys. J.* **403**, 797. DOI: 10.1086/172250
- Wilson, I.R.G.: 2013, *Pattern Recogn. Phys.* **1**, 147. DOI: 10.5194/prp-1-147-2013
- Wolff, C.L., Patrone, P.N.: 2010, *Solar Phys.* **266**, 227. DOI: 10.1007/s11207-010-9628-y
- Wood, K.D.: 1972, *Nature* **240**, 91. DOI: 10.1038/240091a0
- Wood, R.M., Wood, K.D.: 1965, *Nature* **208**, 129. DOI: 10.1038/208129a0
- Yi, W.: 1992, *J. Roy. Astron. Soc. Can.* **86**, 89.
- Zaqarashvili, T.V.: 1997, *Astrophys. J.* **487**, 930. DOI: 10.1086/304629